Biomimetic Materials

DOI: 10.1002/anie.201402608

Polydopamine as a Biomimetic Electron Gate for Artificial Photosynthesis**

*Jae Hong Kim, Minah Lee, and Chan Beum Park**

Abstract: *We report on the capability of polydopamine (PDA), a mimic of mussel adhesion proteins, as an electron gate as well as a versatile adhesive for mimicking natural photosynthesis. This work demonstrates that PDA accelerates the rate of photoinduced electron transfer from light-harvesting molecules through two-electron and two-proton redox-coupling mechanism. The introduction of PDA as a charge separator significantly increased the efficiency of photochemical water oxidation. Furthermore, simple incorporation of PDA ad-layer on the surface of conducting materials, such as carbon nanotubes, facilitated fast charge separation and oxygen evolution through the synergistic effect of PDA-mediated proton-coupled electron transfer and the high conductivity of the substrate. Our work shows that PDA is an excellent electron acceptor as well as a versatile adhesive; thus, PDA constitutes a new electron gate for harvesting photoinduced electrons and designing artificial photosynthetic systems.*

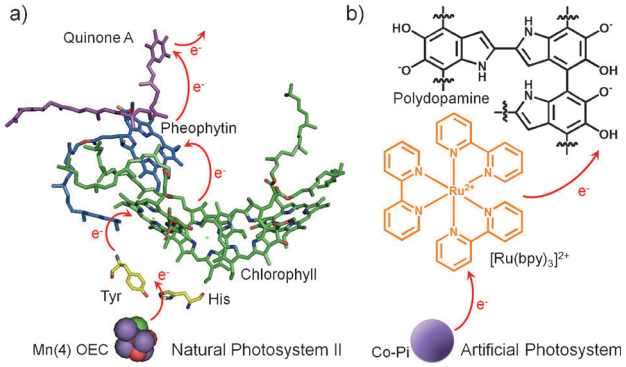

Figure 1. a) Natural photosystem II and b) artificial photosystem composed of PDA (redox mediator), $[Ru(bpy)_3]^{2+}$ (photosensitizer), and Co-Pi (OEC). PDA was introduced to mimic the role of quinone A because of its similarly functioning ligand (i.e., the semiquinone group).

An attractive route for the generation of clean, sustainable energy in the future is the conversion of solar to chemical energy by mimicking natural photosynthesis.[1] An efficient, photoinduced transfer of electrons and protons is crucial for the design of artificial photosynthetic systems.[2] In green plants, photosynthesis occurs through fast charge separation upon photon absorption by the molecular energy transduction complexes that contain photosensitizers and electron acceptors. In particular, quinone molecules, such as primary and secondary acceptor quinone (Q_A and Q_B, repectively), function as redox shuttles for the transfer of two electrons and two protons from chlorophyll molecules through pheophytin in 200 ps.[3] Quinone intermediates (reduced quinones, Q_AH_2 and Q_BH_2) that are formed by accepting electrons and protons drive a long-lived charge separation of chlorophyll with a minimal charge recombination, thus increasing quantum efficiency. As depicted in Figure 1a, the state of charge separation by reduced Q_A and Q_B facilitates a forward electron transfer from the oxygen-evolving center (OEC) through chlorophyll and pheophytin.[4] Recognizing the role of quinone molecules in natural photosynthesis, many researchers attempted to design an efficient donor–acceptor assembly for utilization of solar energy.[5] For example, carbon-based nanomaterials, such as carbon nanotubes (CNTs), were considered as electron acceptors for fast charge transfer from photosensitizers because of their unique properties (e.g., high electron mobility and aspect ratio).[6] However, metallic and bundling properties cause unwanted electron transfer, such as back electron transfer and charge recombination, because of the continuous energy state of CNTs.[7] Thus, proper modification of the CNT surface is critically needed for the generation of new energy states and prevention of bundling without degeneration of their unique electronic properties.[8]

Herein, we report on the use of polydopamine (PDA), a mimic of mussel adhesive proteins that contain 3,4-dihydroxy-L-phenylalanine (DOPA), as an electron gate to imitate the role of quinone molecules in natural photosystem II (Figure 1b). PDA possesses numerous catechol groups that are redox-active functional ligands suitable for a wide range of electrochemical applications, such as biosensors, microbial fuel cells, and Li-ion batteries.[9] PDA can act as an electron acceptor at neutral and basic pH values because of its functional ligands such as semiquinones and quinones (Figure S1, Supporting Information).[10] According to the present work, the charge separation of $[Ru(bpy)_3]^{2+}$, a light-harvesting molecule, is significantly enhanced in the presence of PDA as a result of efficient proton-coupled electron transfer, which is a simultaneous (or sequential) electron transfer from donor to acceptor with protons.[11]

[*] Dr. J. H. Kim, M. Lee, Prof. Dr. C. B. Park
Department of Materials Science and Engineering
Korea Advanced Institute of Science and Technology
335 Science Road, Daejeon 305-701 (Republic of Korea)
E-mail: parkcb@kaist.ac.kr

[**] This study was supported by grants from the National Research Foundation (NRF) through the National Leading Research Laboratory (NRF-2013R1A2A1A05005468), the Intelligent Synthetic Biology Center of Global Frontier R&D Project (2011-0031957), and the Converging Research Center (2013K000236), Republic of Korea.

Supporting information for this article is available on the WWW under http://dx.doi.org/10.1002/anie.201402608.

Thereby, photochemical water oxidation at cobalt phosphate (Co-Pi), a biomimetic OEC,[12] is highly facilitated by the acceleration of photoinduced electron transfer from $[Ru(bpy)_3]^{2+}$ to functional ligands of PDA (e.g., semiquinones, quinones). PDA could further serve as a versatile agent for the surface functionalization of materials without geometric hindrance;[13] it readily forms a thin nanofilm on various types of materials, such as noble metals, oxides, semiconductors, and synthetic polymers, regardless of their size or morphology. We have found that a PDA coating on CNTs significantly improved the efficiency of photoinduced electron transfer and photochemical water oxidation as a result of the synergistic effect of the redox properties of PDA and the high conductivity of CNTs.

We compared the electrochemical properties of PDA with those of quinones by conducting a cyclic voltammetry analysis of PDA using a PDA-coated ITO (indium tin oxide) electrode as a working electrode (Figure 2). We immersed a bare ITO

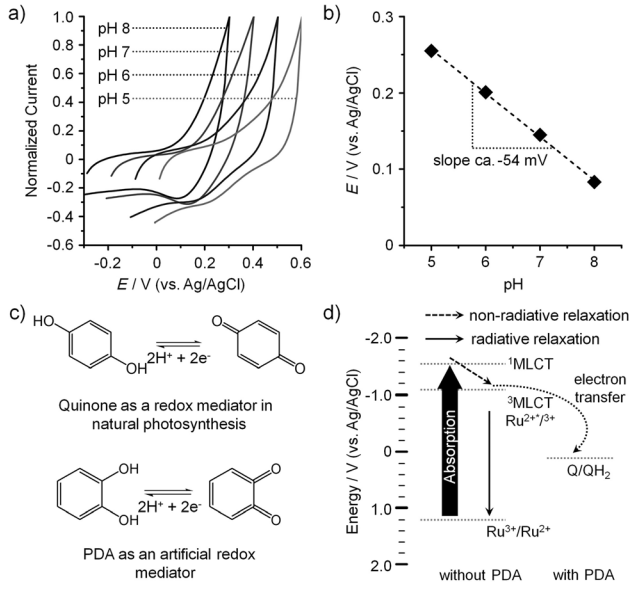

Figure 2. Electrochemical property of PDA-coated ITO electrodes. a) Cyclic voltammogram of PDA-coated ITO electrodes at different pH values. b) Plot of the cathodic potential of PDA-coated ITO electrodes versus the pH value. c) Comparison of the proton-coupled electron transfer between quinone and the catechol groups of PDA. d) Energetic relationship between PDA and $[Ru(bpy)_3]^{2+}$. The charge recombination would be prevented by the electron transfer from $[Ru(bpy)_3]^{2+}$ to PDA. QH_2 and Q represent the catechol group of PDA and its oxidized form, respectively.

electrode in a dopamine solution (1 mg mL^{-1}, pH 8.5) for pH-triggered, oxidative polymerization of catecholamine on the electrode surface (Figure S2). According to the Fourier transform IR spectrum of the PDA-coated ITO electrode (Figure S3a), new peaks were observed at 1280, 1450, 1510, and 3250 cm^{-1} after PDA treatment; the new peaks should originate from phenolic C-O-H stretching, C-C vibration of the benzene ring, amine N-H sharing, and phenolic O-H stretching vibrations, respectively.[14] In addition, new Raman peaks at 1405 and 1590 cm^{-1}, which correspond to aromatic components of PDA,[15] appeared after the polymerization of dopamine, thus indicating the polymerization of dopamine to PDA on the surface of the ITO electrode (Figure S3b). We found that a cathodic current (I_{pc}) for the PDA-coated ITO electrode and its peak (E_{pc}) were proportional to the scan rate and its logarithm, respectively (Figure S4a), in accordance with the redox behavior of an anthraquinone-modified glassy carbon electrode.[16] At scan rates above 200 mV s^{-1}, the degree of peak separation increased, while E_{pc} values were proportional to the logarithm of the scan rate (Figure S4b). Using Laviron's theory, we estimated the electron-transfer rate constant (k_c) and the charge-transfer coefficient (α_c) by plotting peak potential versus scan rate. The values of k_c and α_c were calculated to be 1.85 s^{-1} and 0.12, respectively. These values are comparable to those of dopamine-bound, self-assembled monolayer electrodes,[17] implying that PDA maintained its electrochemical property originated from the catechol groups after self-polymerization of dopamine on the ITO electrode. In addition, the energy level of the E_{pc} of PDA shifted anodically with the decreasing pH value (Figure 2a). The plot of the E_{pc} position as a function of the pH value showed a slope of approximately 54 mV per pH unit (Figure 2b), whereas the theoretical value of catechol for two-electron two-proton redox coupling is around 59 mV per pH unit, according to the literature [18]. In a natural photosystem, quinone molecules function as a two-electron gate, increasing the efficiency of electron transfer from chlorophyll by a factor of two.[3] In a similar way, the abundant catechol groups in PDA can also act as a redox shuttle for the transfer of two protons and two electrons (Figure 2c). Furthermore, the reduction potential of PDA is at 0.07 V (vs. Ag/AgCl) in a phosphate buffer (10 mM, pH 8.0), which is similar to the energy level of Q_A (−0.08 V vs. the normal hydrogen electrode (NHE)). Figure 2d shows the energetic relationship between PDA and $[Ru(bpy)_3]^{2+}$ suggesting that PDA is a biomimetic redox-shuttling chemical for charge separation of a photosensitizer under visible light. In natural photosystem II, the excited electrons of P680 (−0.64 V vs. NHE) are transferred to pheophytin (−0.50 V vs. NHE), which is similar to the electron transfer from the singlet state (^{1}MLCT) of $[Ru(bpy)_3]^{2+}$ to its triplet state (^{3}MLCT).[19] The electrons transferred from P680 to pheophytin are subsequently delivered to Q_A and Q_B, resulting in the formation of Q_AH_2 and Q_BH_2, respectively. Similarly, the reduction potential of PDA is suitable to accept excited electrons from the triplet state of $[Ru(bpy)_3]^{2+}$.

Based on the redox behavior of PDA, we investigated the electron transfer from $[Ru(bpy)_3]^{2+}$ to PDA using cyclic voltammetry. Figure 3a shows the change of voltammetric features of PDA with and without $[Ru(bpy)_3]^{2+}$. The presence of $[Ru(bpy)_3]^{2+}$ significantly improved the I_{pc} of PDA at the reduction potential ($\approx$0.07 V vs. Ag/AgCl, pH 8.0), indicating that the functional groups of PDA gained electrons from $[Ru(bpy)_3]^{2+}$. The current difference between PDA with and without $[Ru(bpy)_3]^{2+}$ was approximately 5 μA, two orders of magnitude higher than the current intensity of $[Ru(bpy)_3]^{2+}$-only ($\approx$0.04 μA; Figure S5). Reports of 2,6-dichloro-1,4-benzoquinone increasing the photocurrent by accepting excited electrons from chlorophyll in photosystem II also

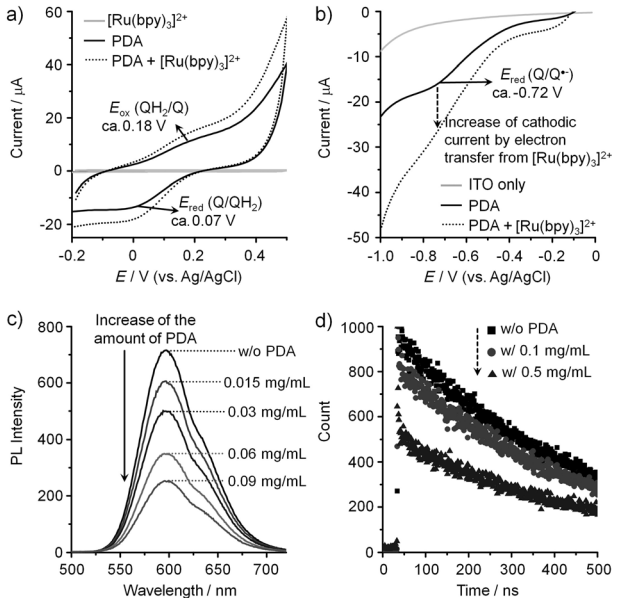

Figure 3. Electron delivery from $[Ru(bpy)]_3^{2+}$ to PDA. a) Cyclic and b) linear-sweep voltammogram of a $[Ru(bpy)_3]^{2+}$-containing phosphate buffer (10 mM, pH 8.0) in the absence and presence of PDA. The potential was scanned at 100 $mV\,s^{-1}$. The redox peaks at 0.07 and 0.18 V (vs. Ag/AgCl) in Figure 3a correspond to the reduction and oxidation of PDA, respectively. In addition, the cathodic peak at −0.72 V is the reduction potential of the quinone group of PDA to form radical quinone anions, according to the literature [20]. c) Changes in the emission spectrum of $[Ru(bpy)_3]^{2+}$ in the presence of various amounts of PDA. d) Photoluminescence decay profiles of $[Ru(bpy)_3]^{2+}$ in the presence of PDA at different concentrations. w/ = with, w/o = without.

mentioned the increased I_{pc}.[21] Furthermore, we found a cathodic wave at −0.72 V (vs. Ag/AgCl, pH 8.0), which is related to the formation of quinone radical anion at −0.45 V (vs. NHE).[22] The position of the cathodic potential is suitable for the oxidative quenching of $[Ru(bpy)_3]^{2+}$ ($0.75\ V > E > -0.85\ V$ (vs. NHE)).[20] This was supported by the increase of the cathodic current of PDA with $[Ru(bpy)_3]^{2+}$ in comparison to PDA-only case (Figure 3b).

An electron is excited to the lowest singlet excited state (^{1}MLCT) of $[Ru(bpy)_3]^{2+}$ at −1.46 V (vs. Ag/AgCl) and then converted to the lowest triplet state (^{3}MLCT) of $[Ru(bpy)_3]^{2+}$ at −1.05 V (vs. Ag/AgCl; see Figure S7). The electron at ^{3}MLCT of $[Ru(bpy)_3]^{2+}$ moves to the quinone groups of PDA at −0.72 V (vs. Ag/AgCl). Eventually, the radical form of the functional groups in PDA is reduced through the coupling of protons at 0.07 V (vs. Ag/AgCl). The gradient of energy potential between $[Ru(bpy)_3]^{2+}$ and PDA should drive efficient electron flow under visible light. To verify the facilitated electron transfer from the ^{3}MLCT state of $[Ru(bpy)_3]^{2+}$ to PDA, we used spectrofluorometric analysis to investigate the efficiency of the PDA-triggered charge separation of $[Ru(bpy)_3]^{2+}$. As shown in Figure 3c, we observed a gradual decrease of emission intensity of $[Ru(bpy)_3]^{2+}$ at 596 nm with an increasing amount of PDA. We attribute this result to the inhibition of the radiative decay of excited electrons in $[Ru(bpy)_3]^{2+}$ by PDA. To further confirm electron delivery from $[Ru(bpy)_3]^{2+}$ to PDA, we measured the photoluminescence lifetimes of $[Ru(bpy)_3]^{2+}$ with and without PDA. The photoluminescence of $[Ru(bpy)_3]^{2+}$ with PDA decayed more quickly than that of free $[Ru(bpy)_3]^{2+}$ (Figure 3d); according to a monoexponential function, the lifetimes of $[Ru(bpy)_3]^{2+}$ with 0.1 and 0.5 $mg\,mL^{-1}$ PDA were 429.9 and 412.8 ns, respectively, while the lifetime of free $[Ru(bpy)_3]^{2+}$ was 444.5 ns, which is a reliable value in comparison with the reported one ($\approx$400 ns) of $[Ru(bpy)_3]^{2+}$ in aerated water at room temperature.[23] Thus, our static and dynamic photoluminescence studies showed that PDA facilitates efficient electron transfer from the ^{3}MLCT state of $[Ru(bpy)_3]^{2+}$ instead of charge recombination. Through spectroscopic and elemental analyses, we calculated the quenching rate constant of $[Ru(bpy)_3]^{2+}$ in the presence and absence of PDA, indirectly comparing the effect of PDA for the charge separation of excited $[Ru(bpy)_3]^{2+}$. According to our calculation, the quenching rate constant of PDA is approximately $1.0\times10^{10}\,M^{-1}s^{-1}$, which is comparable to the reported values for quinone-based quenchers (e.g., $3.7\times10^{9}\,M^{-1}s^{-1}$ for benzoquinone; $2.4\times10^{9}\,M^{-1}s^{-1}$ for trimethylhydroquinone; and $6.0\times10^{9}\,M^{-1}s^{-1}$ for anthraquinone-2,6-disodium sulphonate).[24] Note that the main absorbance of $[Ru(bpy)_3]^{2+}$ at 460 nm was not affected by PDA (Figure S8), which indicates that PDA performs the role of an electron acceptor. Taken together, this shows that PDA acts as an efficient redox mediator to enhance photoinduced electron transfer from $[Ru(bpy)_3]^{2+}$. Note that the quenching rate constant of PDA is higher than that of a cobalt-based water oxidation catalyst, which plays a role as an hole scavenger (i.e., $1.3\times10^{9}\,M^{-1}s^{-1}$ for cobalt-oxo cubane),[25] suggesting that the rate-limiting step in the photochemical water oxidation, such as a reduction half-reaction, would be overcome by the introduction of PDA as an charge separator.

We applied PDA-induced charge separation to photochemical water oxidation using Co-Pi as a biomimetic OEC (similar to the cobalt-oxo cubane)[25] with $[Ru(bpy)_3]^{2+}$ as a photosensitizer under the illumination by visible light ($\lambda >$ 420 nm). We used $Na_2S_2O_8$ as an electron acceptor in a phosphate buffer (10 mM) at pH 8.0. As shown in Figure 4a, the amount of evolved oxygen after 10 min of illumination was approximately 1.65, 2.26, and 3.26 μmol in the presence of 0.005, 0.01, and 0.02 $mg\,mL^{-1}$ PDA, respectively. Accordingly, the turnover number with PDA (0.02 $mg\,mL^{-1}$) was 130.4, approximately twice that without PDA ($\approx$65.2). Moreover, the turnover frequency (TOF $\approx 0.88\ s^{-1}$) in the presence of PDA (0.02 $mg\,mL^{-1}$) was much accelerated in comparison to the $[Ru(bpy)_3]^{2+}$-only case ($0.32\ s^{-1}$). The oxygen evolution rate was proportional to the amount of PDA, indicating that the fast charge separation of $[Ru(bpy)_3]^{2+}$ by PDA facilitated the efficiency of photochemical water oxidation. According to the literature,[21] ITO electrodes modified by quinone derivatives (e.g., 2,6-dichloro-1,4-benzoquinone) promote the turnover number and frequency of photoelectrochemical water oxidation by natural photosystem II. We attribute the improved ability of PDA to take electrons from $[Ru(bpy)_3]^{2+}$ to the deprotonation of catechol groups. To test this theory, we conducted photochemical water oxidation by varying the pH value from 5.0 to 8.0, which is the range for a two-proton-coupled electron transfer by quinones.[26] As shown in Fig-

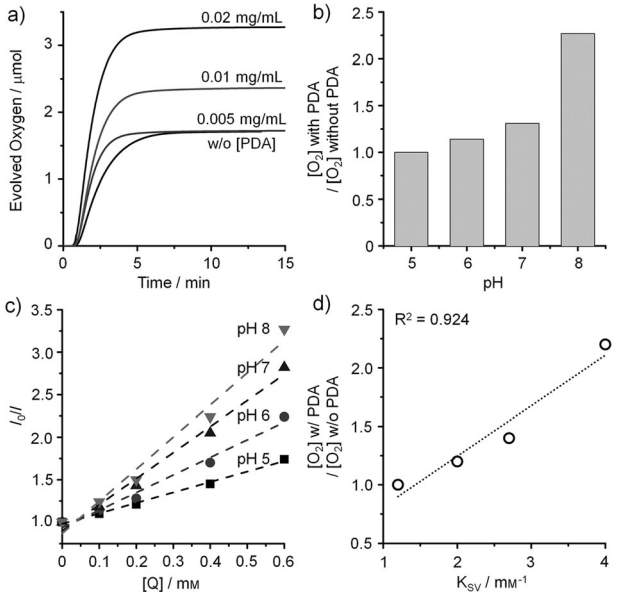

Figure 4. a) Time profiles of oxygen evolution for 0.01 mM Co-Pi with 0.25 mM $[Ru(bpy)_3]^{2+}$ and varying concentrations of PDA in a phosphate buffer at pH 8.0 containing 5 mM sodium persulfate. b) Ratio of the amounts of evolved oxygen with and without PDA at different pH values. c) Stern–Volmer plot for $[Ru(bpy)_3]^{2+}$ in the presence of semiquinone groups of PDA at different concentrations. The concentrations of the semiquinone groups of PDA were determined by elemental analysis. Slopes of Stern–Volmer plot were substantially increased with an increasing pH value. d) Plot showing the relationship between catalytic activity and the Stern–Volmer coefficient (K_{SV}). Catalytic activity was defined as a ratio of oxygen evolution with PDA to that without PDA.

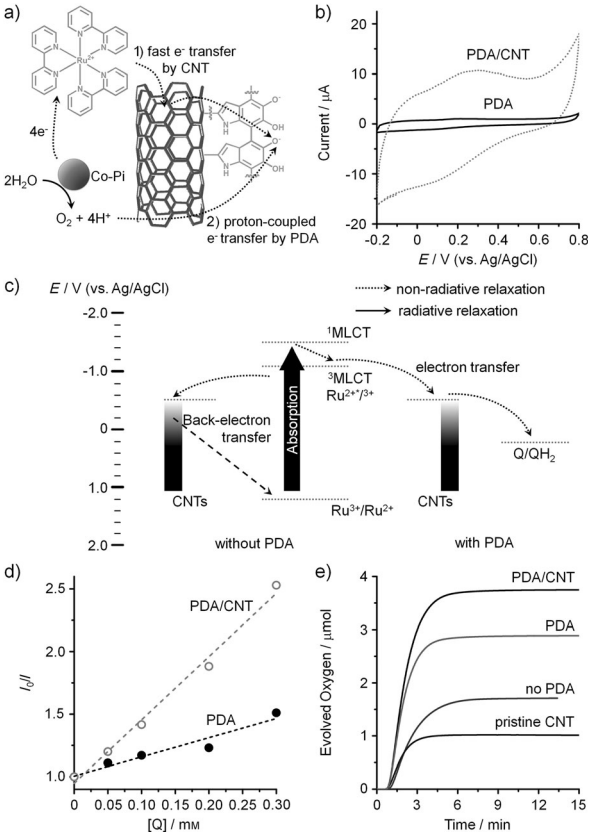

Figure 5. a) Schematic illustration of photochemical water oxidation by Co-Pi, $[Ru(bpy)_3]^{2+}$, and PDA-coated CNTs. b) Cyclic voltammogram of a PDA-only sample and PDA-coated CNTs. c) Comparison between charge separation of $[Ru(bpy)_3]^{2+}$ by CNTs and PDA-coated CNTs. $[Ru(bpy)_3]^{2+}$ absorbs photons and generates excited electrons, which are instantly transferred to the CNTs. In the presence of PDA ad-layer on the surface of CNTs, back-electron transfer from the CNTs to $[Ru(bpy)_3]^{2+}$ is inhibited by the redox behavior of PDA. The energy state of CNTs was adopted from the literature [27]. d) Stern–Volmer plot for $[Ru(bpy)_3]^{2+}$ in the presence of PDA and PDA-coated CNTs at different concentrations. e) Time profiles of oxygen evolution for 0.01 mM Co-Pi with 0.25 mM $[Ru(bpy)_3]^{2+}$ without and with three different additives (0.02 mg mL^{-1} pristine CNTs, PDA, and PDA-coated CNTs) in a phosphate buffer at pH 8.0 containing 5 mM sodium persulfate.

ure 4b, the ratio of evolved oxygen with PDA to that without PDA was substantially enhanced by increasing the pH value. Furthermore, we observed a Stern–Volmer relationship between $[Ru(bpy)_3]^{2+}$ and the catechol groups of PDA by varying the pH value (Figure 4c). The Stern–Volmer coefficient (K_{SV}) was linearly correlated to the pH value, and the ratio of evolved oxygen with PDA to that without PDA exhibited a first-order dependence on K_{SV} (Figure 4d). These data indicate that efficient water oxidation was achieved by the enhanced photoinduced electron transfer between $[Ru(bpy)_3]^{2+}$ and $Na_2S_2O_8$ through the introduction of PDA. Taken together, PDA is shown to be an excellent electron acceptor that can facilitate proton-coupled electron transfer and improve the efficiency of photochemical water oxidation.

We attempted to address the aforementioned problems of CNTs as an electron acceptor in artificial photosynthesis through the coating of PDA, a mussel-inspired universal adhesive, to the surface of CNTs. We expected that the PDA ad-layer on CNTs would reduce unwanted electron transfer caused by the aggregation of metallic CNTs in the donor–acceptor assembly. Furthermore, high conductivity of CNTs can boost the charge transfer from $[Ru(bpy)_3]^{2+}$ to PDA (Figure 5a). The TEM images in Figure S9 show that the CNTs were fully and uniformly covered by the PDA ad-layer with a thickness of approximately 3 nm. According to our cyclic voltammetric analysis (Figure 5b), both cathodic and anodic currents of the PDA-coated CNTs increased at a rate approximately 10 times greater than that of the PDA-only sample, which suggests that CNTs can accelerate the rate of PDA-mediated photoinduced electron transfer from $[Ru(bpy)_3]^{2+}$. This theory was supported by the increased degree of $[Ru(bpy)_3]^{2+}$ quenching by PDA-coated CNTs, as shown in Figure 5d. The K_{SV} of $[Ru(bpy)_3]^{2+}$ with PDA-coated CNTs (4.95 mM^{-1}) was much higher than that of the PDA-only sample (1.68 mM^{-1}).

While the conductivity of the PDA-coated CNTs was slightly reduced from pristine CNTs (Figure S10), the new reduction potential at 0.08 V (vs. Ag/AgCl) from the PDA layer on the surface of CNTs facilitated the formation of energetic charge-separated states of $[Ru(bpy)_3]^{2+}$. Thus, it prevented back-electron transfer from CNTs to $[Ru(bpy)_3]^{2+}$ as a result of the continuous energy states of CNTs as an electron acceptor (Figure 5c). To investigate the synergistic effect of PDA and CNTs on photochemical water oxidation,

we tested three different samples: PDA only, pristine CNTs, and PDA-coated CNTs. We observed that pristine CNTs inhibited the catalytic activity of Co-Pi on photochemical water oxidation (1.01 μmol) compared to the activity without an electron mediator (1.65 μmol) (Figure 5e). According to the literature,[27] a decrease of current density in dye-sensitized solar cells containing metallic CNTs was observed as a result of back-electron transfer from CNTs to the electrolyte and photosensitizer. Thus, we attribute the impediment of oxygen evolution with pristine CNTs to the continuous energy state of metallic CNTs. However, the turnover number and frequency of photochemical water oxidation with the PDA-coated CNTs were 150.5 and 1.01 s^{-1}, respectively, much higher than those of PDA-only samples ($\approx$115.8 and 0.83 s^{-1}) and those without PDA ($\approx$65.2 and 0.34 s^{-1}; Table S1). In addition, the quantum yield of photochemical water oxidation under the irradiation of a blue-light-emitting device ($\lambda \approx 450$ nm $\pm$ 10 nm) with the PDA-coated CNTs ($\approx$6.6%) and PDA ($\approx$5.1%) was much higher than that without PDA ($\approx$3.0%; Table S1), implying that the redox activity of PDA and the high conductivity of CNTs contribute synergistically to the enhanced rate of forward electron transfer with a minimal back-electron transfer. Taken together, PDA is an excellent electron acceptor as well as a versatile adhesive for efficient photoinduced electron transfer.

In summary, we first demonstrated that mussel-inspired PDA is an efficient redox mediator mimicking quinone molecules in natural photosystem II. Our results show that PDA accelerates the rate of photoinduced electron transfer from $[Ru(bpy)_3]^{2+}$ through a two-electron and two-proton redox-coupling mechanism. The introduction of PDA as a charge separator increased the catalytic activity of Co-Pi with $[Ru(bpy)_3]^{2+}$ on photochemical water oxidation by approximately 2.75 times. Furthermore, simple incorporation of a PDA ad-layer onto the surface of CNTs facilitated fast charge separation of $[Ru(bpy)_3]^{2+}$ and efficiency improvement of photochemical water oxidation through the synergistic effect of PDA-mediated proton-coupled electron transfer and the high conductivity of CNTs. Thus, PDA opens a new electron gate for harvesting photoinduced electrons, enabling efficient and forward electron transfer toward realizing artificial photosynthesis.

Received: February 20, 2014
Published online: April 1, 2014

Keywords: biomimetic materials · electron transfer · photosynthesis · polydopamine · water oxidation

[1] a) Y. Tachibana, L. Vayssieres, J. R. Durrant, *Nat. Photonics* **2012**, *6*, 511 – 518; b) G. W. Crabtree, N. S. Lewis, *Phys. Today* **2007**, *60*, 37 – 42.

[2] a) S. H. Lee, J. H. Kim, C. B. Park, *Chem. Eur. J.* **2013**, *19*, 4392 – 4406; b) J. H. Kim, M. Lee, J. S. Lee, C. B. Park, *Angew. Chem.* **2012**, *124*, 532 – 535; *Angew. Chem. Int. Ed.* **2012**, *51*, 517 – 520; c) J. Ryu, S. H. Lee, D. H. Nam, C. B. Park, *Adv. Mater.* **2011**, *23*, 1883 – 1888.

[3] R. E. Blankenship in *Molecular Mechanisms of Photosynthesis*, Blackwell, Hoboken, **2008**, pp. 124 – 156.

[4] I. McConnell, G. H. Li, G. W. Brudvig, *Chem. Biol.* **2010**, *17*, 434 – 447.

[5] J. Wiberg, L. J. Guo, K. Pettersson, D. Nilsson, T. Ljungdahl, J. Martensson, B. Albinsson, *J. Am. Chem. Soc.* **2007**, *129*, 155 – 163.

[6] D. M. Guldi, G. M. A. Rahman, F. Zerbetto, M. Prato, *Acc. Chem. Res.* **2005**, *38*, 871 – 878.

[7] a) F. Bonaccorso, *Int. J. Photoenergy* **2010**; b) M. J. O'Connell, S. M. Bachilo, C. B. Huffman, V. C. Moore, M. S. Strano, E. H. Haroz, K. L. Rialon, P. J. Boul, W. H. Noon, C. Kittrell, J. Ma, R. H. Hauge, R. B. Weisman, R. E. Smalley, *Science* **2002**, *297*, 593 – 596.

[8] a) S. R. Jang, R. Vittal, K. J. Kim, *Langmuir* **2004**, *20*, 9807 – 9810; b) J. X. Geng, B. S. Kong, S. B. Yang, S. C. Youn, S. Park, T. Joo, H. T. Jung, *Adv. Funct. Mater.* **2008**, *18*, 2659 – 2665.

[9] a) Y. Tan, W. Deng, Y. Li, Z. Huang, Y. Meng, Q. Xie, M. Ma, S. Yao, *J. Phys. Chem. B* **2010**, *114*, 5016 – 5024; b) M.-H. Ryou, D. J. Lee, J.-N. Lee, Y. M. Lee, J.-K. Park, J. W. Choi, *Adv. Energy Mater.* **2012**, *2*, 645 – 650; c) T.-T. Zheng, R. Zhang, L. Zou, J.-J. Zhu, *Analyst* **2012**, *137*, 1316 – 1318.

[10] B. Yu, J. Liu, S. Liu, F. Zhou, *Chem. Commun.* **2010**, *46*, 5900 – 5902.

[11] a) D. R. Weinberg, C. J. Gagliardi, J. F. Hull, C. F. Murphy, C. A. Kent, B. C. Westlake, A. Paul, D. H. Ess, D. G. McCafferty, T. J. Meyer, *Chem. Rev.* **2012**, *112*, 4016 – 4093; b) M. H. V. Huynh, T. J. Meyer, *Chem. Rev.* **2007**, *107*, 5004 – 5064.

[12] D. Shevchenko, M. F. Anderlund, A. Thapper, S. Styring, *Energy Environ. Sci.* **2011**, *4*, 1284 – 1287.

[13] a) A. Postma, Y. Yan, Y. Wang, A. N. Zelikin, E. Tjipto, F. Caruso, *Chem. Mater.* **2009**, *21*, 3042 – 3044; b) L. Q. Xu, W. J. Yang, K.-G. Neoh, E.-T. Kang, G. D. Fu, *Macromolecules* **2010**, *43*, 8336 – 8339.

[14] L.-P. Zhu, J.-H. Jiang, B.-K. Zhu, Y.-Y. Xu, *Colloids Surf. B* **2011**, *86*, 111 – 118.

[15] S. H. Ku, C. B. Park, *Biomaterials* **2010**, *31*, 9431 – 9437.

[16] M. A. Ghanem, J. M. Chretien, A. Pinczewska, J. D. Kilburn, P. N. Bartlett, *J. Mater. Chem.* **2008**, *18*, 4917 – 4927.

[17] J.-J. Sun, J.-J. Xu, H.-Q. Fang, H.-Y. Chen, *Bioelectrochem. Bioenerg.* **1997**, *44*, 45 – 50.

[18] H. A. Laitinen, *Chemical Analysis: An Advanced Text and Reference*, McGraw-Hill, New York, **1960**.

[19] Y. Kato, M. Sugiura, A. Oda, T. Watanabe, *Proc. Natl. Acad. Sci. USA* **2009**, *106*, 17365 – 17370.

[20] K. S. Schanze, K. Sauer, *J. Am. Chem. Soc.* **1988**, *110*, 1180 – 1186.

[21] M. Kato, T. Cardona, A. W. Rutherford, E. Reisner, *J. Am. Chem. Soc.* **2012**, *134*, 8332 – 8335.

[22] R. Breslow, *Pure Appl. Chem.* **1974**, *40*, 493 – 509.

[23] a) J. V. Caspar, T. J. Meyer, *J. Am. Chem. Soc.* **1983**, *105*, 5583 – 5590; b) K. J. Morris, M. S. Roach, W. Y. Xu, J. N. Demas, B. A. DeGraff, *Anal. Chem.* **2007**, *79*, 9310 – 9314; c) A. Juris, V. Balzani, F. Barigelletti, S. Campagna, P. Belser, A. von Zelewsky, *Coord. Chem. Rev.* **1988**, *84*, 85 – 277.

[24] J. R. Darwent, K. Kalyanasundaram, *J. Chem. Soc. Faraday Trans. 2* **1981**, *77*, 373 – 382.

[25] M. D. Symes, D. A. Lutterman, T. S. Teets, B. L. Anderson, J. J. Breen, D. G. Nocera, *ChemSusChem* **2013**, *6*, 65 – 69.

[26] W. B. Zhang, S. M. Rosendahl, I. J. Burgess, *J. Phys. Chem. C* **2010**, *114*, 2738 – 2745.

[27] X. Dang, H. Yi, M.-H. Ham, J. Qi, D. S. Yun, R. Ladewski, M. S. Strano, P. T. Hammond, A. M. Belcher, *Nat. Nanotechnol.* **2011**, *6*, 377 – 384.

